https://doi.org/10.46813/2022-140-061

SURFACE MODIFICATION OF THE TITANIUM ALLOY VT22 BY HIGH CURRENT PULSED ELECTRON BEAM

S.Ye. Donets[1], V.V. Lytvynenko[1], Yu.F. Lonin[2], A.G. Ponomarev[2], O.A. Startsev[1], V.T. Uvarov[2]
[1]Institute of Electrophysics and Radiation Technologies National Academy of Science of Ukraine, Kharkiv, Ukraine;
[2]NSC "Kharkov Institute of Physics and Technology", Kharkiv, Ukraine
E-mail: vvlytvynenko@ukr.net

The industrial Titanium VT22 alloy was irradiated using the high-current pulsed electron beam (HCEB). HCEB method is an effective method to test the materials under extreme volumetric thermo-mechanical and irradiation conditions. The intense electron irradiation resulted in evolution of microstructural composition. It was found that formation of the β-phase, whereas nonirradiated material consists α+β-phases. The corresponding temperature field and mechanical displacement fields were calculated using the finite-element thermoelastic model.

PACS: 41.75.Ht, 44.90.+c, 61.05.cp, 81.40.Wx

INTRODUCTION

The titanium alloys are used in aircraft building due to their high strenght, heat resistance, corrosion resistance and serviceability [1]. The VT22 alloy is the metastable near – β titanium alloy Ti-5Al-5Mo-5V-1Cr-1Fe, with traces of <0.3 Zr, < 0.15 Si, < 0.1 C, wt.%. This alloy is used by the Antonov aircraft manufacturing company brand. It was developed in 1960s as a high-strength material to design critical parts to withstand high loads. Its strength reaches up to 1.1 GPa which is achieved by thermal treatment by formation of the bi-phase structure.

High-current relativistic electron beam irradiation is an advanced testing tool [2]. Its relativistic energy provides the volumetric heating in the materials. For example, the peak of maximal temperatures due to the energy loss is below the surface, at around 100…200 μm in pure Titanium for 0.3 MeV electrons. Also, the irradiation induces very high speed of heating (up to 10^9 K/s) and cooling [3]. The irradiated volumes are no longer small as the impacting beam has typically 500…3000 A current. The released energy provokes a deeper heating, high mechanical stresses to accommodate the ablation processes which results in a splash of the vapor-droplet cloud. Having irradiated the sample, the material is quickly recrystallized if the target has an effective thermal contact with the accelerator's collector. This subsequent high-speed crystallization of the melt makes it possible to form a submicron-nanocrystalline structure characterized by a high degree of uniformity in the distribution of chemical elements on the surface layer [4]. Typically, the HCEB accelerators provide microsecond or sub-microsecond duration of impulses. Comparing the HCEB exposure with the laser irradiation, the former provides volumetric heating while the latter has surface effect [5]. However, both of the tools are effective tools for testing the physical properties, while the laser processing is cheaper due to significantly lower infrastructure and maintenance costs, thus, it is more popular tool. HCEB were also a popular tool for a set of problems in plasma domain.

This research is a continuation of the initial research published in [6]. The aim of the current work is to provide further findings revealed with advances in investigations.

1. MATERIALS AND METHODS

The industrial as-received roles of the VT22 alloy were used to cut the plates for samples. The thickness of plates was 3 mm. All surfaces before irradiation were mechanically polished with 12 μm polish paper. For the consecutive irradiations, only one side was irradiated. The methodology and details of the irradiation is described in [6].

The specimens were irradiated at the TEMP-A pulsed e-beam accelerator in the NSC "Kharkov Institute of Physics and Technology". The parameters of the beam were the following: the current of 2 kA, electron energy ~ 350 keV, impulse duration $\tau_p \sim 5$ μs, in vacuum at ~ 10^{-5} Torr. The samples were irradiated sequentially up to 3 impulses in total.

Having received the irradiated samples, smaller pieces were prepared from the cross-section in the epicenter of the impact for metallographic investigations using light microscopy, fractographic analyses, scanning electron microscopy, and H_{200} Vickers microhardness testing. The samples were prepared in the epicenter of irradiation. They were fractured first at liquid nitrogen temperature, and then cut using a wire saw under water cooling.

In order to investigate the details of the crystal structure before and after irradiation, X-ray diffractometry was performed using the Shimadzu XRD-6100 X-ray diffractometer in a scanning range $2\theta = 35…90°$. CrystalDiffract software program (v6.9.3 trial) was used to simulate the diffraction patterns for Titanium and to compare with the observed data [7]. Crystallographic information files 9016190 and 9012924 were taken for a mixture pattern simulation from [8]. It helped to identify the corresponding phases and their peak positions for qualitative phase analysis. Quantitative phase analyses were not possible due to low quality of prepared samples and technical limitations of the diffractometer.

2. NUMERICAL MODELLING

Prior to performing the experiments with irradiation of the specimens, the temperature field and mechanical displacements evolution was simulated to assist the experiments. Numerical modelling of the HCEB irradiation on the VT22 alloy was done using the finite element and finite difference approach which was previously described in [9]. The numerical model is built on top of the hyperbolic Maxwell – Cattaneo – Lykov law for heat conductance, Stefan problem and the weakly coupled dynamic theory of thermoelasticity. The main difference with previous modelling attempts, is the Stefan boundary condition is no longer taken into account as the numerical model is ineffective with tracing the phase-transition boundaries.

The free software package FreeFem v4.11 for partial differential equations was used to perform the modeling [10]. The FD-method was applied to discretize the time operators and the FE-method was used for space discretization. The volumetric heat source releases the energy in the target material over time, the temperature and the fields of displacements are being calculated iteratively until the end of irradiation τ_p.

The initial formulation of the numerical thermoelastic model is computationally expensive and leads to instabilities and multiple numeric approximations. The boundary-tracing method is not possible in a general variational form. Thus, the initial thermoelastic model was simplified for smoothed or constant thermo-mechanical properties of the target, aka single-phase approach in the variational form. This approach has its limitation naturally but results in faster calculations. Also, we introduce a higher penalty by terms of the absorption coefficient ϵ of 0.6 (compared to typical 0.8–0.9) taken in a heat function. This is necessary as the current sample is being irradiated 3 times consecutively which leads to the higher crater effect when the gas-droplet cloud is shielding the epicenter of the heat release.

The corresponding physical and mechanical parameters of the VT22 alloy were taken for simulations from the literature data provided in [11]. The material parameters used in the calculations as per [9] are: $c = 600$ J·kg^{-1}·K^{-1}, $\rho = 4600$ kg·m^{-3}, $k = 14$ W·m^{-1}·K^{-1}, Young's modulus $E = 110$ GPa, Poisson's ratio $\nu = 0.32$, $\alpha_T = 8\cdot10^{-6}$ K^{-1}, $\eta_{eff} = 1.2$, $\epsilon = 0.6$, $\tau_p = 5\cdot10^{-6}$ s, $\tau_r = 10^{-12}$ s, $m = 1$, $\varepsilon_R = 0.5$, $\sigma_R = 6\cdot10^{-8}$ W·m^{-2}·K^{-4}, $H_x = 1.7\cdot10^{-3}$ m, $H_y = 8\cdot10^{-3}$ m, $J = 2\cdot10^3$ A, $U = 0.35$ MeV, $\xi_y = 4\cdot10^{-3}$ m, and $\xi_t = 2\cdot 10^{-6}$ s.

Figs. 1 and 2 illustrate the results of the numerical modelling for the single impact. The numerical simulation of the HCEB irradiation were performed only for the impact of one impulse. As the delay between consecutive 3 irradiations to charge the capacitors was around 15 min, thus, the target cooled due to heat transfer the firmly attached collector. Also, the crater depth after a single impact is in a range of hundreds of micrometers, thus we can consider the target as a new plate. The actual experiment leads to a crater and formation of the relatively rough droplet surface, but we are neglecting those effects in the epicenter of the impact when the droplet-like surface is least pronounced due to tangential component of release of the ablated droplet matter. The highest calculated temperatures in the epicenter were around 2000 °C at 5 μs from the start of irradiation (see Fig. 1). The near-surface layer was melted up to the depth of around 600 μm.

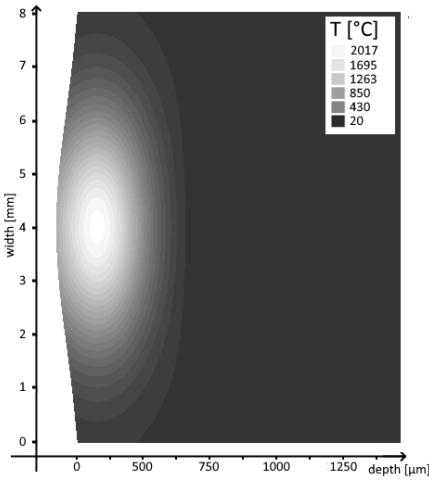

Fig. 1. Temperature distribution in Titanium VT22 at the end of HCEB exposure

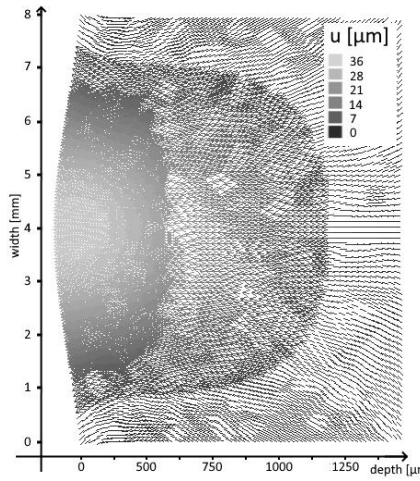

Fig. 2. Vectors of displacements in Titanium VT22 at the end of HCEB exposure

High mechanical stress was observed in the irradiated material, which led to displacements (see Fig. 2). The calculated mass loss per impact is ~ (0.1±0.03) g/impulse, which correlate with previously calculated results in [9].

3. RESULTS AND DISCUSSION

Fig. 3 shows the microstructure of sample before and after the irradiation. There was a significant microstructural modification. Metallographic analyzes revealed the formation of the heat-affect or quenched zone (HAZ). Fig. 3,a illustrates a typical structure in HAZ after the HCEB irradiation with 3 impulses. HAZ has the lamellar-dendritic microstructure with the grains in the direction of the thermal flow. The dendrites were formed as elongated crystallites of primary crystallization during solidification from the liquid phase. Appearance of this microstructure was driven by the thermal flow into the bulk and by the small tangent component of the mass transfer. The dendritic microstructure is homogeneous until the boundary with the non-melted material (see Fig. 3,b) which is observed at the depth around 600 μm from the surface.

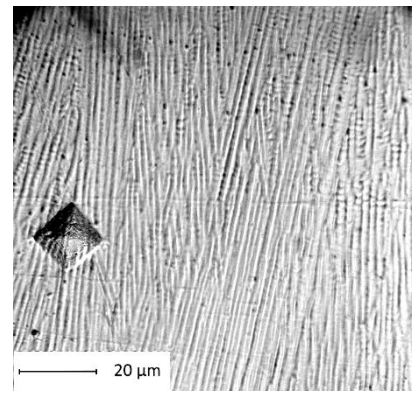

a

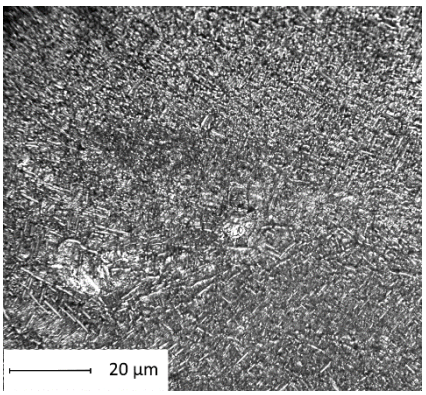

b

Fig. 3. Light optical micrographs of the VT22 alloy after the HCEB irradiation: a – heat-affected remelted zone; b – the non-irradiated reference material

Having compared with the literature data [12, 13], it was deduced that the reference base metal consists of the mixed tempered structure of the very fine acicular martensite α and the fine lamella substructure $\alpha+\beta$. The high contrast on the light microscopy images for the base reference material is explained by the smaller grains and high boundary complexity, and their relatively high disorientation in the parent β-grains. The recrystallized material in HAZ has an ordered structure with larger grains, which led to brighter contrast during chemical etching.

Qualitative XRD analyses were performed on the samples from the irradiated area of remelted zone and from the reference material (Fig. 4). It was confirmed, the reference material contains both α and β-phases. Meanwhile, the remelted material consists of β-phase. It is known, a β-transition temperature of VT22 is around 850 °C [14]. Thus, the fast cooling prevented $\beta \rightarrow \alpha + \beta$ transformation. As cooling is very fast, the formation α-phase is hindered as it required more moderate cooling rates. It was observed from the metallographic analyses, that the interface between the remelted and the reference materials was clearly distinct due to contrast in the microstructures, it means that the thermal flux did not affect the metastable reference material in general. The reference material behaved as a high-capacity thermal sink. This is mainly due to high concentration of alloying elements which stabilizes the solid solution during heat treatments and deformations. Actual macroscopic modification of the microstructure is limited primarily to the remelted layer. It can be speculated, that some decomposition of the bi-phase solution happened in the reference base, but it was not confirmed by the XRD analyzes. Only some tracing of coarsening of the microstructure was observed on the metallographic images in the reference material however it had irregular character.

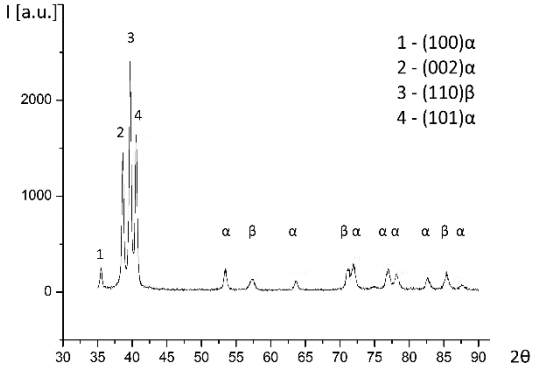

a

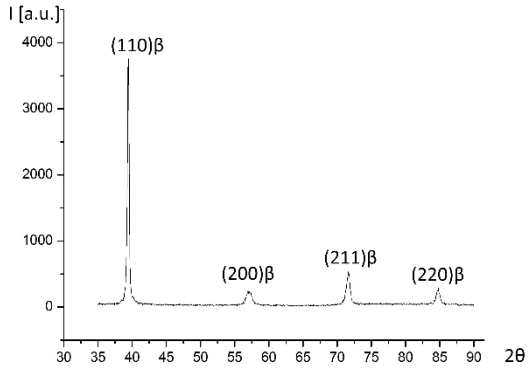

b

Fig. 4. XRD patterns for the samples from the reference base material with minor peaks marked per phase α or β (a) and from the irradiated remelted zone (b)

The mechanical characteristics of irradiated material of the VT22 alloy are significantly lower compared to the reference base metal. Firstly, its microhardness $H_{200}^0 \sim (6.5 \pm 0.3)$ GPa drops to $H_{200}^0 \sim (5.7 \pm 0.3)$ GPa. The decrease in hardness is explained by the formation of the β-phase dendritic microstructure in the melted layer. It is hypothesized that low microhardness is attribute of moderate interface strengthening.

The substantial change of the microfracture mode from ductile to quasi-brittle was concluded from the fractographic analyses. Fig. 5 illustrates fractures of the irradiated sample. We observed formation of the quenched and HAZ on the surface which typical elements of brittle fractures. Important, that the adhesion of the remelted layer to the base reference material is relatively poor as major cracks were observed during mechanical fracture (see Fig. 5,a). Small submicron-sized particles were notices on the interfaces of fractures in the HAZ, but they did not cause a effective hindering of cracks as the latter propagated into the depth of material perpendicularly to the surface of irradiation. This is a typical change of the chemical composition and mechanical properties as can be seen on other materials [15, 16]. The main driving factor of those changes are parameters under which recrystallization occurs.

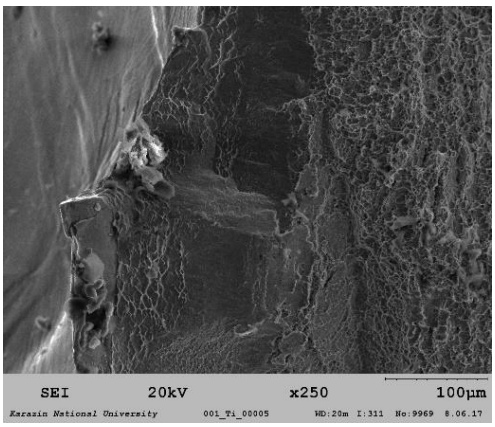

a

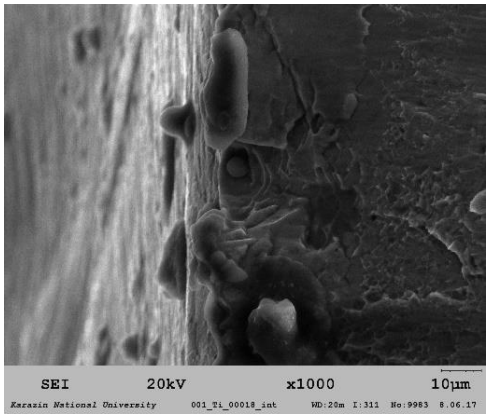

b

Fig. 5. SEM images of fractures in the irradiated zone. The bright-contrast surface on the left is the exposed target surface of the sample

The initially reported decrease in the mass loss from 0.13 g/impulse after the first impulse to 0.07 g/impulse after the 2nd impulse in [9], which was speculated to be attributed to the pronounced crater effect, realistically has a different nature. The modelling underestimation is caused not only by the effects of melt dynamics and back condensation in a crater. The nature should be coming also from the microstructural composition of the sample irradiated with multiple impulses. On the surface of the samples, a thin layer of β-phase is being formed. Normally, the amount of this remelted layer is small after 1 impulse. However, its amount increases with sequential irradiation thus more β-phase is under exposure. The interface between the remelted material and the base metal is prone to cracking, which is an additional factor for faster removal under HCEB. As the HCEB irradiation provokes high temperatures and mechanical stresses, the previously remelted material is partially pilled off from the peripheries of the crater and back-condensed on the target, hence, leaving less to the environment. This combined effect of the crater and the microstructural composition was also observed on the the smaller sample after 3 impulses. It had a higher mass loss due to a greater degree of freedom for the ejection of the melt due to the smaller crater effect and inability to back-condense the previously remelted material.

4. CONCLUSIONS

The high-current pulsed electron-beam irradiation of the industrial wrought titanium alloy VT22 was performed in this study. It was concluded, that the irradiation induces brittleness of the newly formed microstructure. The nature of this is explained by the formation of β-phase in the heat-affected layer compared to α+β-mixed phase of the reference material.

ACKNOWLEDGEMENTS

The authors of this article express appreciation for the funding provided by the National Academy of Sciences of Ukraine to carry out the research program.

REFERENCES

1. I. Inagaki et al. *Application and Features of Titanium for the Aerospace Industry.* 2014.
2. V.F. Klepikov et al. Dynamics of the gas-plasma torch formed by the high-current electron beam action on solid targets // *Problems of Atomic Science and Technology. Series "Plasma Physics" (15).* 2009, N 1, p. 119-121.
3. Chen Li et al. Surface alloying of gray cast iron with chromium by high current pulsed electron beam treatment // *Mater. Res. Express*. 2018, v. 5, N 5.
4. Y. Geng et al. Ultrafast microstructure modification by pulsed electron beam to enhance surface performance // *Surface and Coatings Technology*. 2022, v. 434.
5. J. Santos Solheid et al. Laser surface modification and polishing of additive manufactured metallic parts // *Procedia CIRP*. 2018, v. 74, p. 280-284.
6. S.Ye. Donets et al. Modification effects of microsecond high current Electron beam exposure on titanium VT22 alloy // *Problems of Atomic Science and Technology. Series "Physics of Radiation Effect and Radiation Materials Science" (112)*. 2019, N 4, p. 174-178.
7. CrystalDiffract®, User's guide. 2020.
8. Crystallography Open Database, http://www.crystallography.net/cod/search.html
9. V.F. Klepikov et al. Physical and mechanical properties of titanium alloy VT1-0 after high-current electron beam irradiation // *Problems of Atomic Science and Technology. Series "Physics of Radiation Effect and Radiation Materials Science" (96)*. 2015, N 2, p. 39-42.
10. F. Hecht. New development in FreeFem++ // *Journal of Numerical Mathematics*. 2012, v. 20, N 3-4, p. 251-266.
11. V.N. Moiseev. High strength titanium alloys in aircraft construction // *Tech Light Alloys*. 2002, N 4, p. 77-80.
12. K. Savage. Effect of Carbon on Primary Alpha Percentage in Ti-6Al-4V as Temperature Approaches the Beta Transus // *BSc Thesis*. California Polytechnic State University, 2013, p. 9-14.
13. I.M. Pohrelyuk et al. The influence of rolling modes during deformation-diffusion treatment on wear resistance of VT22 titanium // *Problems of Friction and Wear*. 2017, v. 1(74), p. 5.
14. O.P. Karasevskaya et al. Deformation behavior of beta-titanium alloys // *Materials Science and Engineering: A*. 2003, v. 354, issue 1-2, p. 121-132.

15. V.V. Bryukhovetsky et al. The features of the structural state and phase composition of the surface layer of aluminum alloy Al-Mg-Cu-Zn-Zr irradiated by the high current electron beam // *Nuclear Instruments and Methods in Physics Research, Section B.* 2021, v. 499, p. 25-31.

16. V.F. Klepikov et al. Behavior of Zr1%Nb alloy under swift Kr ion and intense electron irradiation // *Journal of Nano- and Electronic Physics*. 2015, v. 7, issue 4.

Article received 30.06.2022

ПОВЕРХНЕВА МОДИФІКАЦІЯ ТИТАНОВОГО СПЛАВУ ВТ22 СИЛЬНОСТРУМОВИМ ІМПУЛЬСНИМ ЕЛЕКТРОННИМ ПУЧКОМ

С.Є. Донець, В.В. Литвиненко, Ю.Ф. Лонін, А.Г. Пономарьов, О.А. Старцев, В.Т. Уваров

Промисловий титановий сплав ВТ22 опромінено сильнострумовим імпульсним електронним пучком (НСЕВ). Метод НСЕВ є ефективним для випробування матеріалів у екстремальних об’ємних термомеханічних і опромінюваних умовах. Інтенсивне електронне опромінення призвело до еволюції мікроструктури. Встановлено, що у переплавленому шарі спостерігається утворення β-фази, тоді як неопромінений матеріал містив α+β-фазу. За допомогою термопружної моделі методом скінченних різниць було розраховано відповідні температурне поле та поле механічного зміщення.